

SUPPLEMENTARY INFORMATION

Development of CHARMM-CER force field:

The *CHARMM-CER* forcefield was constructed based on the CHARMM all-atom force field.¹⁻³ While lipid parameters in CHARMM exist, they have not been derived specifically for ceramide (CER) lipids and no parameters are explicitly given for the amide group found in CERs, shown in Figure 2 of the main document. In order to determine the missing parameters, *ab initio* calculations were performed to obtain missing force constants and the equilibrium bond distances/angles in atomistic CER NS and NP molecules. The electron structure was also obtained to determine the atomic partial charges on the corresponding atoms. Dihedral parameters and van der Waals interactions were used directly from the peptide bond parameters in the CHARMM protein force field¹. The sources for this extended version of the force field are summarized in Table S1.

Table S1. Force field development for CER lipids (*CHARMM-CER*)

Interactions	Hydrocarbon Tails	Hydroxyl Group	Amide Group
Bonds and Angles	CHARMM36 lipid topology	CHARMM36 lipid topology	<i>ab initio</i> calculation
Dihedrals	CHARMM36 lipid topology	CHARMM36 lipid topology	CHARMM36 protein force field, peptide group
van der Waals	CHARMM36 lipid topology	CHARMM36 lipid topology	CHARMM36 protein force field, peptide group
Partial charges	Quantum mechanics <i>ab initio</i> calculation		

Bonded interactions:

To calculate the missing bonded parameters, *i.e.*, bond stretching and angle bending, the molecular software package GAUSSIAN 09⁴ was used to perform *ab initio* calculations with the B3LYP level of theory and the 6-31++G** basis set.

Eight random configurations of each molecule were generated with the molecular editor software package Avogadro^{5,6}. Since internal CH₂ groups along the tails are expected to contain a total neutral charge and the longest-range bonded interaction is a 1-4 dihedral, the CER molecules were truncated to tails of four carbons in length. The structure of the truncated CER NS is shown in Figure S1. A geometric optimization was then performed on each of the eight input data files to determine the equilibrium configuration, from which the force constants and equilibrium distances/angles were averaged; these values are reported in Table S2. Again, dihedral parameters were taken from the peptide bond in the CHARMM protein force field¹.

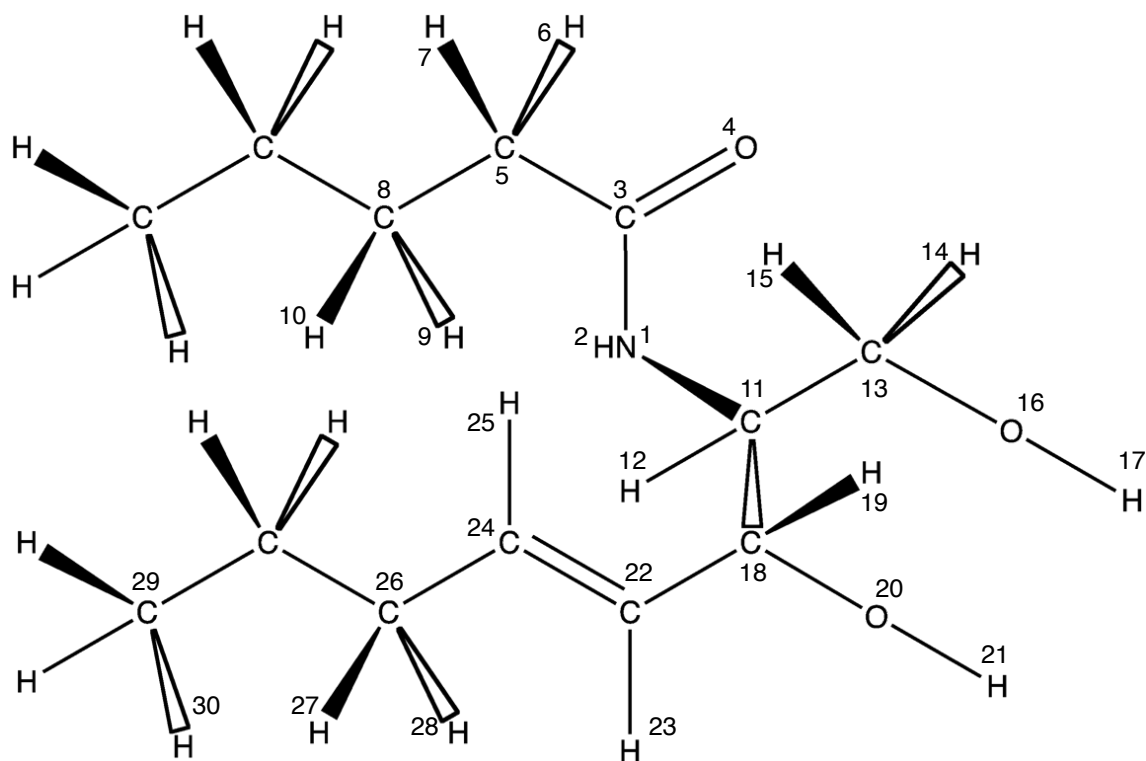


Figure S1. Structure of the truncated CER NS used in the *ab initio* calculation.

Table S2. Bond and angle parameters from *ab initio* calculation for the amide group. Atom index 1, 2, 3 and 4 are the nitrogen, hydrogen, carbon and oxygen in the amide group; atom index 11 is the carbon connected with the amide group to the phytosphingosine/sphingosine tail.

Amide bonded interactions	BOND	
	Force constant (kcal/mol/ \AA^2)	Equilibrium bond length (\AA)
N-H (1-2)	537.50	1.0108
N-C (1-3)	506.50	1.3659
N-C (1-11)	371.95	1.4668
C=O (3-4)	875.00	1.2302
C-C (3-5)	315.45	1.5269
ANGLE		
	Force constant (kcal/mol/radian ²)	Equilibrium angle (degree)

N-C=O (1-3-4)	178.500	122.44
H-N-C (2-1-3)	78.875	119.61
H-N-C (2-1-11)	35.000	116.55
C-N-C (3-1-11)	108.500	123.36
N-C-C (1-3-5)	155.400	115.48
O-C-C (4-3-5)	203.100	118.09

Non-bonded interactions

The same eight random configurations, as used in the discussion above, were also used to determine the point charges of isolated CER NS and NP molecules. Single-point energy calculations were performed on the eight input data files and the partial charges subsequently obtained using the Mulliken population analysis. The results (shown for CER NS in Table S3) were averaged over all eight data files to obtain the partial charge for each atom. The structure and partial charges of the CER NS and NP molecules are shown in Figure 1 of the main document.

Table S3. Partial charge calculation results for truncated CER NS. Atom index is as that shown in Figure S1.

Index	Atom	Run 1	Run 2	Run 3	Run 4	Run 5	Run 6	Run 7	Run 8	Ave.	StdDev
1	N	-0.54	-0.55	-0.52	-0.53	-0.52	-0.52	-0.52	-0.53	-0.53	1.15E-02
2	H	0.26	0.26	0.27	0.25	0.26	0.26	0.26	0.26	0.26	3.94E-03
3	C	0.57	0.61	0.58	0.63	0.62	0.56	0.56	0.57	0.59	2.64E-02
4	O	-0.52	-0.52	-0.53	-0.52	-0.52	-0.54	-0.52	-0.53	-0.53	5.87E-03
5	C	-0.26	-0.26	-0.26	-0.28	-0.26	-0.25	-0.27	-0.28	-0.27	1.21E-02
6	H	0.13	0.12	0.13	0.14	0.13	0.12	0.13	0.13	0.13	5.72E-03
8	C	-0.17	-0.18	-0.17	-0.17	-0.17	-0.17	-0.18	-0.18	-0.18	4.51E-03
9	H	0.10	0.09	0.10	0.09	0.09	0.09	0.09	0.09	0.09	3.62E-03
11	C	0.05	0.05	0.05	0.03	0.02	0.03	-0.01	0.05	0.03	2.22E-02
12	H	0.11	0.13	0.11	0.12	0.11	0.12	0.11	0.13	0.12	1.30E-02
13	C	0.05	0.06	0.04	0.08	0.07	0.08	0.06	0.06	0.06	1.38E-02
14	H	0.08	0.09	0.12	0.10	0.11	0.11	0.10	0.11	0.10	1.31E-02
16	O	-0.56	-0.56	-0.55	-0.55	-0.55	-0.55	-0.56	-0.55	-0.55	5.34E-03
17	H	0.34	0.34	0.34	0.35	0.34	0.34	0.33	0.33	0.34	7.23E-03
18	C	0.13	0.13	0.13	0.15	0.16	0.18	0.17	0.14	0.15	1.86E-02
19	H	0.07	0.08	0.09	0.08	0.09	0.08	0.07	0.08	0.08	9.16E-03
20	O	-0.58	-0.57	-0.55	-0.54	-0.54	-0.56	-0.58	-0.56	-0.56	1.52E-02
21	H	0.34	0.34	0.34	0.34	0.34	0.34	0.34	0.35	0.34	8.39E-03

22	C	-0.10	-0.09	-0.09	-0.11	-0.09	-0.10	-0.07	-0.10	-0.09	9.95E-03
23	H	0.10	0.09	0.10	0.09	0.09	0.09	0.09	0.09	0.09	3.81E-03
26	C	-0.21	-0.21	-0.21	-0.20	-0.22	-0.23	-0.22	-0.22	-0.22	1.37E-02
27	H	0.10	0.10	0.11	0.12	0.11	0.11	0.10	0.10	0.11	5.65E-03
29	C	-0.32	-0.31	-0.30	-0.29	-0.32	-0.29	-0.30	-0.30	-0.30	1.03E-02
30	H	0.09	0.10	0.09	0.10	0.09	0.10	0.09	0.10	0.10	4.08E-03

Similar to the dihedral interactions, the van der Waals interactions for the amide group were taken from analogous parameters for atoms in a peptide bond as reported in the CHARMM protein force field¹. All other head group dispersion parameters are available in the CHARMM lipid force field².

Structural metrics

Bilayer thickness

Several methods exist in the literature for measuring the bilayer thickness, (note, in all cases, z corresponds to the normal to the bilayer), including (1) measurement of the average z position of phosphates in each leaflet⁷, (2) measurement of the distance between electron density peaks in z direction⁸, and (3) calculation of the interface thickness which refers to the distance over which water density falls from 90% to 30% of bulk value⁹. In the systems studied here, since the highest z position for the head groups in the CERs varies between CER NS and NP, we determine the bilayer height by calculating the interface thickness. The bilayer thickness is extracted from the difference in z -values where water density drops to $1/e$ of its bulk value,¹⁰ as illustrated in Figure S2.

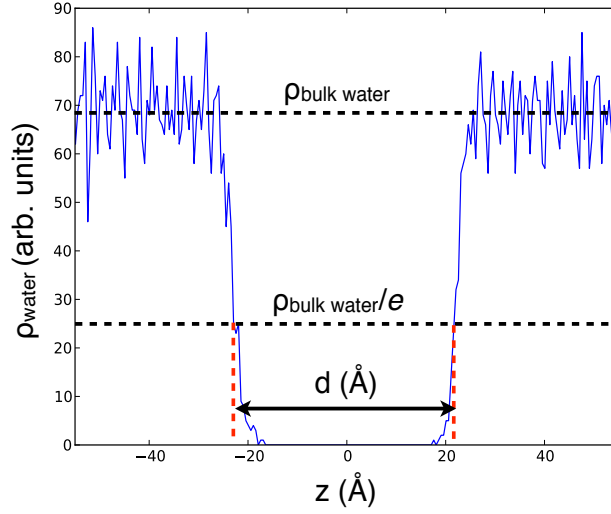


Figure S2. Measurement of bilayer thickness based on the water density profile.

Tail order parameter

To quantify the orientational order of the tail groups in a given leaflet, the nematic order parameter, S_2 ,¹¹ typically used for liquid crystalline systems, is calculated. First, the average direction of each lipid tail is quantified by calculating the moment of inertia tensor of the carbon backbone (or a subset of the carbon backbone in specific cases):

$$I_{\alpha\beta} = \sum_{i=1}^{N_l} m_i \sum \hat{\mathbf{r}}_i^2 \delta_{\alpha\beta} - \mathbf{r}_{i\alpha} \mathbf{r}_{i\beta} \quad , \quad (1)$$

where $\hat{\mathbf{r}}_i$ is the position vector of each particle i relative to the center of mass, and m_i is the mass of each particle i , $\delta_{\alpha\beta}$ is the Kronecker delta, N_l is the total number of particles in the tail segment, and α and β are looping variables that correspond to the coordinate axes (i.e., x , y , z). The characteristic vector describing the tail, $\hat{\mathbf{u}}$, is the eigenvector associated with the smallest eigenvalue of the moment of inertia tensor. These vectors are used to construct the nematic tensor:

$$Q_{\alpha\beta} = \frac{1}{N_L} \sum_{i=1}^{N_L} \frac{3}{2} \mathbf{u}_{i\alpha} \mathbf{u}_{i\beta} - \frac{1}{2} \delta_{\alpha\beta} \quad , \quad (2)$$

where N_L is the total number lipid tails considered. The director of the system is the eigenvector associated with the largest eigenvalue of Q , and the nematic order parameter, S_2 , corresponds to this largest eigenvalue of Q . S_2 can also be defined as,

$$S_2 = \langle \frac{3}{2} \cos^2 \theta - \frac{1}{2} \rangle \quad , \quad (3)$$

where θ is the angle between a tail's principal axis and the preferred direction (i.e., director) of the system and the angle brackets denote an ensemble average. A value of $S_2 = 1$ indicates a perfect nematic crystal; in bilayers system, a fluid bilayer typically has a value of $S_2 < 0.8$, as determined by visual inspection. While in a free polymer system, a disordered fluid state would typically have a value of $S_2 < 0.3$, the interface between the lipids and water in the CER system induces increased nematic ordering, even for systems that are not very well ordered (hence, the larger value). Note, each leaflet in the bilayer is considered separated, as the orientation may differ, and the two values averaged.

Tilt angle

Tilt angle is defined as the deviation of the system director (described above) from the vector normal to the bilayer interface; in this case, the normal is assumed to be parallel with the z-axis of the coordinate frame.

Planar order parameter

To determine the degree of 2d crystalline ordering between the tails in the bilayer plane, a global order parameter is constructed using the superposition method, outlined in references.^{12, 13} Briefly, the center of mass of each of the tails is calculated and projected onto the xy plane, where each leaflet is considered separately. Using these centers of mass, the nearest neighbor shell surrounding a given tail is determined. The collection of local clusters are then translated to a common origin, constructing what is commonly termed a bond-order diagram; systems with long range crystalline ordering will show correlations between nearest neighbor directions in this diagram. The bond order diagram is then converted to a scalar order parameter by taking the magnitude Fourier transform with a given frequency. In the case of hexagonal ordering, the 6th frequency is used, which results in an order parameter from 0 to 1, with a maximum value of unity for ideal hexagonal crystalline packing. Note that this is different from taking the average of the first neighbor hexagonal ordering (i.e., the average value of the fourier transform of each cluster), since in that case, collective orientational ordering is not preserved during the calculation, and thus long range order cannot be assessed. The metric considered here, relying on superposition, enables the collective, long-range ordering to be determined.

References

1. MacKerell, A. D.; Bashford, D.; Bellott, M.; Dunbrack, R. L.; Evanseck, J. D.; Field, M. J.; Fischer, S.; Gao, J.; Guo, H.; Ha, S.; Joseph-McCarthy, D.; Kuchnir, L.; Kuczera, K.; Lau, F. T. K.; Mattos, C.; Michnick, S.; Ngo, T.; Nguyen, D. T.; Prodhom, B.; Reiher, W. E.; Roux, B.; Schlenkrich, M.; Smith, J. C.; Stote, R.; Straub, J.; Watanabe, M.; Wiorkiewicz-Kuczera, J.; Yin, D.; Karplus, M., All-atom empirical potential for molecular modeling and dynamics studies of proteins. *Journal of Physical Chemistry B* **1998**, *102* (18), 3586-3616.

2. Klauda, J. B.; Venable, R. M.; Freites, J. A.; O'Connor, J. W.; Tobias, D. J.; Mondragon-Ramirez, C.; Vorobyov, I.; MacKerell, A. D.; Pastor, R. W., Update of the CHARMM All-Atom Additive Force Field for Lipids: Validation on Six Lipid Types. *The Journal of Physical Chemistry B* **2010**, *114* (23), 7830-7843.
3. Pastor, R. W.; MacKerell, A. D., Development of the CHARMM Force Field for Lipids. *J. Phys. Chem. Lett.* **2011**, *2* (13), 1526-1532.
4. M. J. Frisch, G. W. T., H. B. Schlegel, G. E. Scuseria, M. A. Robb, J. R. Cheeseman, G. Scalmani, V. Barone, B. Mennucci, G. A. Petersson, H. Nakatsuji, M. Caricato, X. Li, H. P. Hratchian, A. F. Izmaylov, J. Bloino, G. Zheng, J. L. Sonnenberg, M. Hada, M. Ehara, K. Toyota, R. Fukuda, J. Hasegawa, M. Ishida, T. Nakajima, Y. Honda, O. Kitao, H. Nakai, T. Vreven, J. A. Montgomery, Jr., J. E. Peralta, F. Ogliaro, M. Bearpark, J. J. Heyd, E. Brothers, K. N. Kudin, V. N. Staroverov, R. Kobayashi, J. Normand, K. Raghavachari, A. Rendell, J. C. Burant, S. S. Iyengar, J. Tomasi, M. Cossi, N. Rega, J. M. Millam, M. Klene, J. E. Knox, J. B. Cross, V. Bakken, C. Adamo, J. Jaramillo, R. Gomperts, R. E. Stratmann, O. Yazyev, A. J. Austin, R. Cammi, C. Pomelli, J. W. Ochterski, R. L. Martin, K. Morokuma, V. G. Zakrzewski, G. A. Voth, P. Salvador, J. J. Dannenberg, S. Dapprich, A. D. Daniels, Ö. Farkas, J. B. Foresman, J. V. Ortiz, J. Cioslowski, and D. J. Fox, Gaussian 09, Revision A.1. In *Gaussian, Inc.*, Wallingford CT: 2009.
5. Avogadro: an open-source molecular builder and visualization tool. Version 1.03. <http://avogadro.openmolecules.net/>.
6. Hanwell, M.; Curtis, D.; Lonie, D.; Vandermeersch, T.; Zurek, E.; Hutchison, G., Avogadro: an advanced semantic chemical editor, visualization, and analysis platform. *Journal of Cheminformatics C7 - 17* **2012**, *4* (1), 1-17.
7. Reddy, A. S.; Warshaviak, D. T.; Chachisvilis, M., Effect of membrane tension on the physical properties of DOPC lipid bilayer membrane. *Biochimica et Biophysica Acta (BBA) - Biomembranes* **2012**, *1818* (9), 2271-2281.
8. Garidel, P., Structural organisation and phase behaviour of a stratum corneum lipid analogue: ceramide 3A. *Physical Chemistry Chemical Physics* **2006**, *8* (19), 2265-2275.
9. Notman, R.; den Otter, W. K.; Noro, M. G.; Briels, W. J.; Anwar, J., The Permeability Enhancing Mechanism of DMSO in Ceramide Bilayers Simulated by Molecular Dynamics. *Biophysical Journal* **2007**, *93* (6), 2056-2068.
10. Das, C.; Noro, M. G.; Olmsted, P. D., Simulation Studies of Stratum Corneum Lipid Mixtures. *Biophysical Journal* **2009**, *97* (7), 1941-1951.
11. Wilson, M. R., Determination of order parameters in realistic atom-based models of liquid crystal systems. *J. Mol. Liq.* **1996**, *68* (1), 23-31.
12. Keys, A. S.; Iacovella, C. R.; Glotzer, S. C., Characterizing complex particle morphologies through shape matching: Descriptors, applications, and algorithms. *Journal of Computational Physics* **2011**, *230* (17), 6438-6463.
13. Keys, A. S.; Iacovella, C. R.; Glotzer, S. C., Characterizing Structure Through Shape Matching and Applications to Self-Assembly. In *Annual Review of Condensed Matter Physics, Vol 2*, Langer, J. S., Ed. 2011; Vol. 2, pp 263-285.